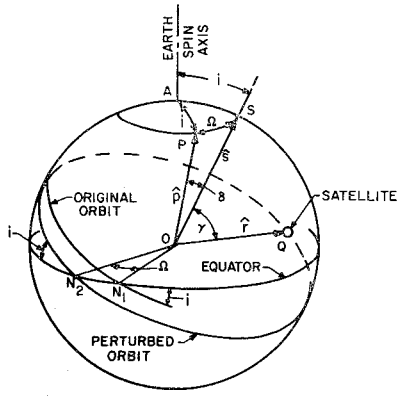

Fig. 2 Unit sphere showing original and perturbed orbits.

For a fixed value of α_1, it is seen that this inequality may be satisfied only for values of i below a certain critical value. To find this critical value, note that the left-hand side of inequality (8) is a minimum when $\Omega = 180°$, so that the critical value of i occurs at

$$\cos^2 i - \sin^2 i = \cos 2i = \sin\alpha_1 \qquad (9)$$

This last result shows that an isotropic antenna is necessary if $\cos 2i < \sin\alpha_1 = \cos(90° - \alpha_1)$, or if

$$i > 45° - (\alpha_1/2) \qquad (10)$$

This shows that isotropic antennas are required for all inclinations over 45° and many orbits below 45°, depending on altitude. For example, an altitude of 6000 miles above the earth's surface corresponds to $\alpha_1 = 23.5°$. Thus, all orbits at this altitude with an inclination in excess of $i = 45° - 11.75° = 33.25°$ require an isotopic antenna for complete earth coverage at all times. For lower inclinations, the required angle may be found from Eq. (7) or from Fig. 3, which shows how the required tolerance angle $\alpha_T = \alpha - \alpha_1$ varies with inclination and regression of the node Ω.

Finally, from Eq. (7), it is seen that (if $i < 45° - \alpha_1/2$) the maximum value of α occurs when Ω is 180°, and the required antenna angle is given by

$$2\alpha_{max} = 2[90° + \alpha_1 - \text{arc sin}(\cos 2i)] = 2\alpha_1 + 4i \qquad (11)$$

and $2\alpha_{max} = 180°$ for $i > 45° - \alpha_1/2$.

For nearly polar orbits, the regression rate of the orbital plane is quite low, since it is proportional to the cosine of the inclination of the orbital plane.[1] For 6000-mile orbits the regression rate is only 2.5°/yr/deg off the polar orbital plane. Therefore, for satellites of finite service life of, for example, 5–10 yr, it is possible to acquire both antenna gain and complete earth coverage. To show this in a specific way on 6000-mile nearly polar orbits, Eq. (7) is plotted in Fig. 4, taking into account an initial injection tolerance (assumed to be 2°). It is noted from Fig. 4 that for orbits within 5° from the polar plane the toroidal antenna pattern will continue to illuminate the visible earth for at least 5 yrs.

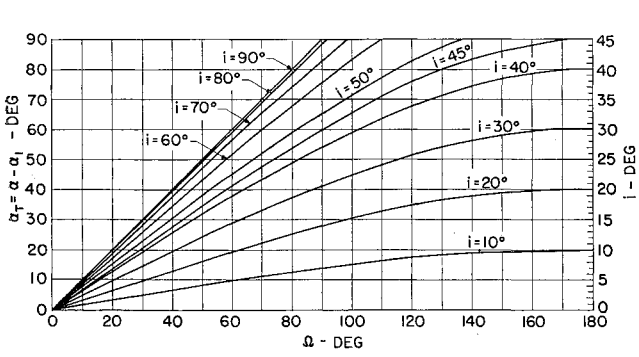

Fig. 3 Tolerance angle α_T vs position of orbital node Ω for various angles of inclination i.

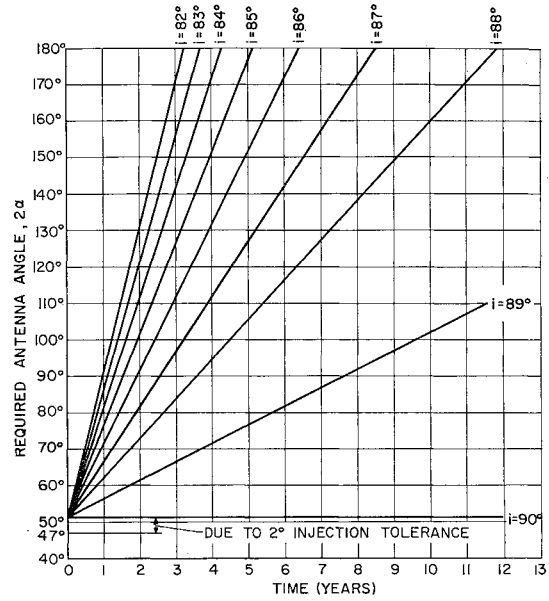

Fig. 4 Required antenna angle for complete coverage at 6000-mile altitude and various orbital inclinations, including effect of 2° injection error and orbital precession.

Reference

[1] Blanco, V. M. and McCuskey, S. W., *Basic Physics of the Solar System* (Addison-Wesley Publishing Co. Inc., Reading, Mass., 1961), p. 202.

Mach Number Independence of the Conical Shock Pressure Coefficient

Glen W. Zumwalt* and H. H. Tang†
Oklahoma State University, Stillwater, Okla.

Nomenclature

C_p = pressure coefficient
K = constant
M = Mach number
P = static pressure
q = dynamic pressure
ϵ = density ratio [Eq. (2)]
θ = conical angle (semivertex)
γ = specific heat ratio

Subscripts

∞ = freestream conditions
c = conditions on the cone surface
w = conditions immediately downstream of the conical shock wave

A SIMPLE relationship exists for conical shocks which, to the authors' knowledge, has not been pointed out before and for which no complete explanation is readily found. This relationship concerns the pressure coefficient across a conical shock produced by air (a perfect gas) flowing at zero

Received March 27, 1963; revision received July 15, 1963. The work reported in this paper was performed in connection with research sponsored by Sandia Corporation, Albuquerque, N. Mex.

* Associate Professor of Mechanical and Aerospace Engineering. Member AIAA.
† Instructor in Aerospace Engineering. Member AIAA.

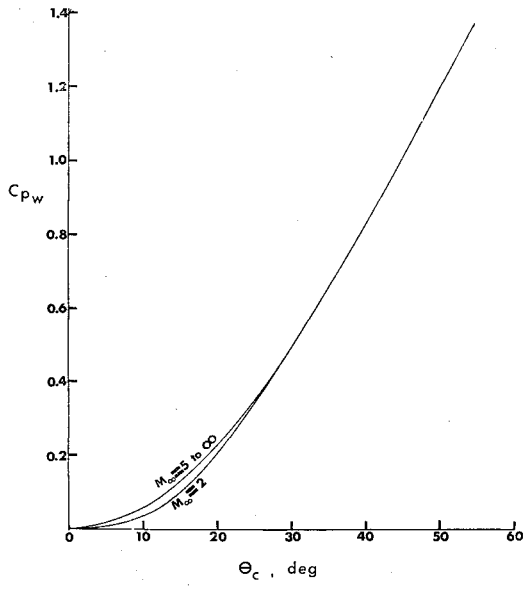

Fig. 1 Pressure coefficient behind a conical shock wave as a function of the cone semi-apex angle.

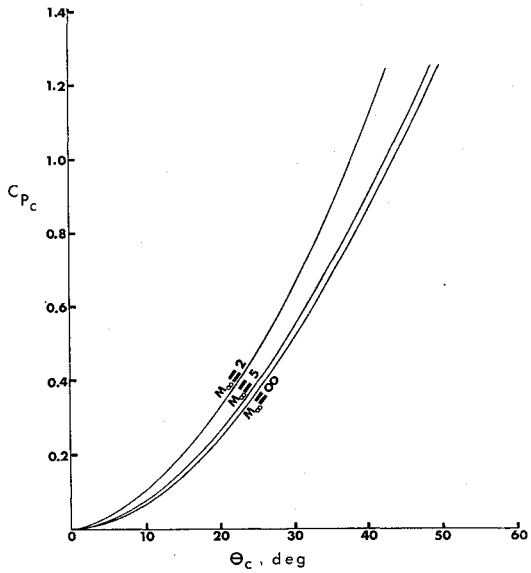

Fig. 2 Pressure coefficient on a cone surface as a function of the cone semi-apex angle and flight Mach number.

yaw angle to a cone surface. The across-shock pressure coefficient is found to be almost entirely independent of the freestream Mach number, being a function only of the cone angle, as shown in Fig. 1.

Although some Mach number independence is to be expected under hypersonic conditions, in this case the independence sets in at surprisingly low Mach numbers. Consider, for example, the cone surface pressure coefficient. From Fig. 2, it can be seen that C_{p_c} is still a function of Mach number for the same range of conditions.

For a partial explanation of this effect, consider the hypersonic case. At hypersonic Mach numbers, the "constant density approximation" can be employed in the thin shock layer. Following the method of Ref. 1,

$$C_{p_w} = 2(1 - \epsilon)\sin^2\theta_w \tag{1}$$

$$\epsilon = \frac{\rho_\infty}{\rho_w} = \frac{2(\theta_w - \theta_c)}{\tan\theta_w} \tag{2}$$

Combining these,

$$C_{p_w} = 2\left[1 - \frac{2(\theta_w - \theta_c)}{\tan\theta_w}\right]\sin^2\theta_w \tag{3}$$

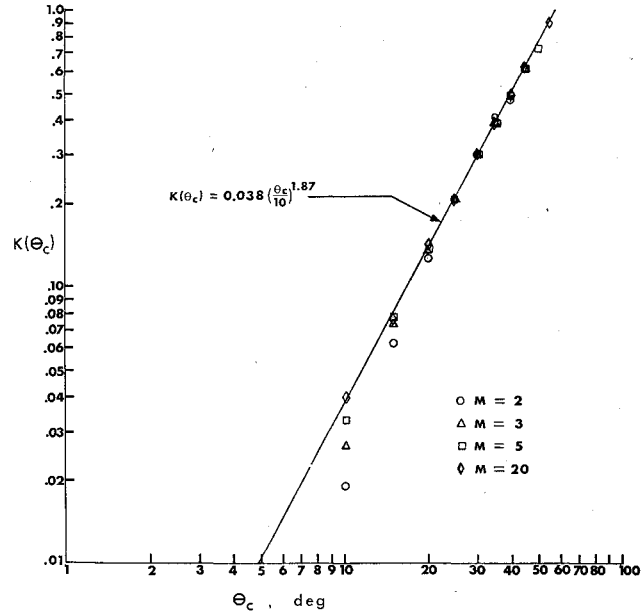

Fig. 3 Plot of K (θ_c) vs cone semi-apex angle.

But θ_w is an implicit function of θ_c, as can be seen by combining equations in Hayes' and Probstein's analysis[1]:

$$\sin\theta_c = \left(1 - \frac{\theta_w - \theta_c}{\tan\theta_w}\right)\sin\theta_w \cos(\theta_w - \theta_c) \tag{4}$$

Therefore, $C_{p_w} = f(\theta_c)$ only. This function is, however, difficult to isolate in the foregoing equations. Although the foregoing is derived for hypersonic flow, Van Dyke[2] has shown that the surface pressure coefficient maintains the same similitude into the lower (supersonic) range. It may be suspected, then, that the shock pressure coefficient will behave similarly, and this appears to be true.

The unique dependence of the shock pressure coefficient on cone angle can be used to derive a simple expression for conical shock angle as a function of cone angle and Mach number. Such an expression can be used in analytical work to replace the usual tabular or graphical representations. The pressure rise coefficient

$$C_{p_w} \equiv (P_w - P_\infty)/q_\infty \tag{5}$$

across a conical (locally, a plane) shock is given by

$$C_{p_w} = \frac{4}{\gamma + 1}\left(\sin^2\theta_w - \frac{1}{M_\infty^2}\right) \tag{6}$$

If $C_{p_w} = f(\theta_c)$, then $[\sin^2\theta_w - (1/M^2_\infty)]$ also must be simply a function of θ_c. Thus, for a given cone angle,

$$\sin^2\theta_w - (1/M^2_\infty) = \text{const} = K(\theta_c) \tag{7}$$

$$\sin\theta_w = K(\theta_c) + (1/M^2_\infty) \tag{8}$$

The value of $K(\theta_c)$, calculated from published values of θ_w,[3] is shown in Fig. 3. Approximating the curve as

$$K = 0.038(\theta_c/10)^{1.87} \tag{9}$$

where θ_c is in degrees, one has the closed-form expression for shock angle:

$$\sin\theta_w = [0.038(\theta_c/10)^{1.87} + (1/M^2_\infty)]^{1/2} \tag{10}$$

For $M_\infty \gg 1$, this results in the same functional relationship as that resulting from the hypersonic "constant density" analysis, Eq. (4).

The simplicity of this expression can be appreciated by comparison with the oblique shock equation for these same three variables suggested by Thompson[4] and recommended in

Ref. 3. This involves a cubic equation in $\sin^2\theta_w$, with surface angle and M_∞ appearing in the coefficients.

The shock-wave angles given by Eq. (10) differ from those calculated by Kopal[5] as follows: for $M_\infty = 3$ and $\theta_c = 42°$, difference less than 1°; for $M_\infty > 3$ and $\theta_c < 42°$, difference less than $\frac{1}{2}°$; and for $\theta_c > 42°$, poor agreement.

This last restriction is not serious, since the maximum possible θ_c for attached conical shock is 49.3° at $M_\infty = 3$ and rises to 56.7° at $M_\infty = 10$.

The shock angle relation provides a possible simplification for computing methods, such as that suggested by Miles[6] for finding properties in the flow field behind a conical shock.

References

[1] Hayes, W. D. and Probstein, R. F., *Hypersonic Flow Theory* (Academic Press, New York, 1959), p. 146.

[2] Van Dyke, M. D., "The combined supersonic-hypersonic similarity rule," J. Aeronaut. Sci. **18**, 499–500 (1951).

[3] Ames Research Staff, "Equations, tables, and charts for compressible flow," NACA Rept. 1135 (1953).

[4] Thompson, M. J., "A note on the calculation of oblique shock-wave characteristics," J. Aeronaut. Sci. **17**, 741–744 (1950).

[5] Kopal, Z., "Tables of supersonic flow around cones," TR 1, Center of Analysis, Mass. Inst. Tech. (1947).

[6] Miles, E. R. C., *Supersonic Aerodynamics* (Dover Publications, New York, 1950), pp. 192–195.

Laminar Flow in Plane Wakes of a Conducting Fluid in the Presence of a Transverse Magnetic Field

A. S. GUPTA*

Indian Institute of Technology, Kharagpur, India

IT is well known that flows in wakes arising out of the separation of the fluid from an obstacle on both sides tend to be turbulent as the Reynolds number R exceeds about 1000. This tendency increases with increasing R. In the case of a flat plate, although the boundary layer remains laminar as far as the trailing edge for $R < 10^6$, the flow in the wake still becomes turbulent. The reason for this, perhaps, lies in the circumstance that velocity profiles in the wake, all of which possess a point of inflexion, are extremely unstable. If, however, the fluid is electrically conducting and a magnetic field is present, transition to turbulence may be delayed due to the stabilizing influence of the field, and a laminar flow presumably may be maintained in the wake.

Using Oseen's approximation, Tollmien[1] obtained the velocity distribution (based on similarity considerations) in the plane laminar wake behind a drag-producing body at a large distance from the body. Recently, Mellor[2] has given a general solution to the laminar flow in wakes and has shown that Tollmien's solution is the leading term of a more general series solution and represents the asymptotic behavior of the wake at a large distance from the body. Mellor's solution includes the case of a wake behind a self-propelled body as discussed by Birkhoff and Zarantonello.[3] In this note, Tollmien's solution will be extended to the case of an electrically conducting fluid when a transverse magnetic field is present, using Mellor's approach. The induced magnetic field is neglected in the analysis, and this is justified for low magnetic Reynolds number, which often is the case in most aerodynamic applications, as pointed out by Resler and Sears.[4] Since the laminar wake is reached by fluid particles that move along streamlines passing fairly close to the body, boundary-layer approximations are valid for this stratum of fluid.

The x axis is taken along the direction of the incident stream moving with velocity U, and a magnetic field $H_0(x)$ is applied perpendicular to this direction, with the origin somewhere in the body. As the electric field $\mathbf{E}$ satisfies curl $\mathbf{E} = 0$ in the steady state, E_z is constant (E_0, say), the z axis being at right angles to the XY plane. Inside the wake, a current is induced in the z direction due to the interaction of the fluid with the magnetic field. Neglecting the induced field and using $j_z = \sigma(E_0 - \mu u H_0)$ from the z component of Ohm's law, the body force $\mu\mathbf{j} \times \mathbf{H}$ has the following components:

$$(\mu\mathbf{j} \times \mathbf{H})_x = \sigma(E_0 H_0 - \mu^2 u H_0^2) \qquad (\mu\mathbf{j} \times \mathbf{H})_y = 0 \quad (1)$$

where μ and σ are the magnetic permeability and electrical conductivity respectively.

The steady boundary-layer equations are now

$$u\frac{\partial u}{\partial x} + v\frac{\partial u}{\partial y} = -\frac{1}{\rho}\frac{\partial p}{\partial x} + \nu\frac{\partial^2 u}{\partial y^2} + \frac{\sigma}{\rho}(E_0 H_0 - \mu^2 u H_0^2) \quad (2)$$

$$0 = \partial p/\partial y \quad (3)$$

where the other components of Maxwell's equations become redundant in view of the foregoing simplifying assumptions. Determining $-(1/\rho)\cdot\partial p/\partial x$ from the freestream value and introducing Oseen's approximation $u = U + u_1$ and $v = v_1$, where u_1 and $v_1 \ll U$, Eq. (2) becomes

$$U\frac{\partial u_1}{\partial x} = \nu\frac{\partial^2 u_1}{\partial y^2} - \frac{\sigma\mu^2 H_0^2(x)}{\rho}u_1 \quad (4)$$

The boundary conditions are $\partial u_1/\partial y = 0$ at $y = 0$ and $u_1 \to 0$ as $y \to \infty$.

Now seek solutions of the form

$$u_1 = a(x)\cdot f(\eta) \qquad \eta = y/C(x) \quad (5)$$

Inserting (5) in (4) yields, after some rearrangement,

$$f'' + \eta f'\cdot\left(\frac{UCC'}{\nu}\right) - \left(\frac{Ua'C^2}{\nu a}\right)f - \left(\frac{\sigma\mu^2 H_0^2(x)\cdot C^2}{\rho\nu}\right)f = 0 \quad (6)$$

where a prime denotes differentiation with respect to the similarity variable η. It is clear from (6) that, for similarity solutions, coefficients within the parentheses of various terms in (6) must be constants. Hence one sets

$$UCC'/\nu = 2 \qquad UC^2a'/\nu a = -4\lambda \qquad \mu^2 H_0^2(x)\cdot C^2 = C_1 \quad (7)$$

The first two equations of (7) give

$$C^2 = 4\nu x/U \qquad a = Ax^{-\lambda} \quad (8)$$

and the last equation gives

$$H_0(x) \sim x^{-1/2} \quad (9)$$

Thus a constant magnetic field evidently precludes affinely similar velocity profiles, and a similarity solution is possible only when $H_0(x)$ behaves like (9). Equation (6) now reduces to

$$f'' + 2\eta f' + 4\lambda' f = 0 \quad (10)$$

where

$$4\lambda' = 4\lambda - (\sigma c_1/\rho\nu) \quad (11)$$

Equation (10) with the boundary conditions $f' = 0$ at $\eta = 0$ and $f = 0$ at $\eta = \infty$ constitutes a Sturm-Liouiville problem with eigenfunctions $f_{\lambda'}$ and eigenvalues λ'.

Putting $\xi = \eta^2$ and $f(\eta) = g(\xi)$, Eq. (10) becomes

$$\xi g'' + (\tfrac{1}{2} + \xi)g' + \lambda' g = 0 \quad (12)$$

Received April 29, 1963.

* Lecturer, Department of Mathematics.